JOURNAL OF CATALYSIS **171,** 383–390 (1997)
ARTICLE NO. CA971814

Selective Oxidation of *n*-Butane to Maleic Anhydride on Vanadyl Pyrophosphate

I. Influence of Oxidation Pretreatments on the Catalytic Performances

K. Aït-Lachgar, M. Abon,[1] and J. C. Volta

Institut de Recherches sur la Catalyse, CNRS, 2 avenue Albert Einstein, 69626 Villeurbanne, France

Received April 14, 1997; revised June 26, 1997; accepted June 30, 1997

A pure and well-crystallized $(VO)_2P_2O_7$ catalyst was oxidized under an oxygen flow at 500°C for different times up to 24 h. These samples were characterized by TGA–DTA, XRD, UV–VIS spectroscopy, and ^{31}P NMR. Their catalytic performances were compared in the selective oxidation of *n*-butane to maleic anhydride (MA) as a function of the time of oxidizing pretreatments. The sample oxidized for 1 h displayed an important increase in MA selectivity (from 52 to 84%), whereas the activity remained virtually nonaffected. These results have been discussed in relation with the development of a proper density of selective V^V species associated with the creation of structural disorder in the pyrophosphate lattice.

INTRODUCTION

The partial oxidation of *n*-butane to maleic anhydride (MA) on V–P–O catalysts is the only example of the oxidation of a light alkane which is industrially performed. Many papers and reviews (1–3) have already been devoted to this complex reaction and catalytic system. However, the nature of the active phase and more precisely the effect of V^V phosphate species on the vanadyl pyrophosphate (V^{IV}) is still debated. Vanadyl pyrophosphate is the only phase usually detected by XRD on long-term equilibrated catalysts (1–5). For this reason it has been frequently proposed that the best V–P–O catalysts only contain well-crystallized $(VO)_2P_2O_7$, as again recently concluded by Guliants *et al.* (6). These authors (6) further claimed that microdomains of δ- and γ-$VOPO_4$ were detrimental to catalyst performances. Bordes and Contractor (7) also considered that orthophosphate phases are harmful although the damages were not too strong with δ- and γ-$VOPO_4$ phases able to be reduced to $(VO)_2P_2O_7$. Centi *et al.* (8) even concluded that V^V ions would be "parasitic species" responsible for the consecutive overoxidation of MA to CO_x. Conversely, Volta *et al.* (9–11) using *in situ* Raman spectroscopy and ^{31}P NMR techniques claimed that more or less disorganized γ-, and δ-, and $\alpha_{\|}$-$VOPO_4$ structures on the $(VO)_2P_2O_7$ matrix would be responsible for the formation of maleic anhydride. δ-$VOPO_4$ is progressively transformed into $\alpha_{\|}$-$VOPO_4$ under catalytic conditions (9, 12). Hutchings and Higgins (13) recently proposed that the specific activity of V–P–O catalysts was controlled mainly by the $\alpha_{\|}$-$VOPO_4$ content.

Using a pulse TAP (temporary analysis of products) reactor, Schuurman *et al.* and Schuurman and Gleaves (14, 15) reported that "reactor equilibrated" $(VO)_2P_2O_7$-based catalysts yielded an increasing rate of MA formation with a better selectivity when previously submitted to oxygen treatments. Coulston *et al.* (16), using time-resolved X-ray absorption spectroscopy, recently concluded that V^{5+} species are kinetically significant for the production of MA. Koyano *et al.* (17, 18), using Raman Spectroscopy, claimed that the oxidation of $(VO)_2P_2O_7$ was anisotropic: the (100) face was oxidized to a selective X_1 phase and the side faces to α- and β-$VOPO_4$. The *n*-butane conversion was over 80% for the first pulse with a selectivity for MA of 13%.

This literature survey shows that several recent studies (9–19) suggest that V^V species on $(VO)_2P_2O_7$ could be beneficial for the selective oxidation of *n*-butane. However, the precise effect of such species (on the conversion or the selectivity), the nature of the desired V^V species (a specific $VOPO_4$ phase or more or less dispersed entities) the optimal V^V/V^{IV} balance, the respective role of V^V and V^{IV} species, and their relative dispersion are still open to discussion. We have therefore investigated the effect of oxidizing treatments on the catalytic performances of a vanadium pyrophosphate catalyst. We prepared first a pure and well-crystallized $(VO)_2P_2O_7$ material (V^{IV} phase) as a standard catalyst. It is already well known that such a solid is quite stable against oxidation. Indeed, high-temperature treatments yield to $VOPO_4$ phases but we did not want to

[1] To whom correspondence should be addressed. Fax: 33 (0) 472 44 53 99.

0021-9517/97 $25.00

achieve complete oxidation to δ-, γ-, or β-$VOPO_4$ phases already studied by Zhang-Lin *et al.* (19). The aim was to perform a mild and controlled oxidation of $(VO)_2P_2O_7$. It may be recalled that it is well accepted that the selective face is the (100) cleavage plane (2–4, 20, 21) but Volta *et al.* (10) proposed that a suitable amount of V^V species (either dispersed V^V sites or small $VOPO_4$ domains) must be present in this (100) face to ensure the selective formation of MA.

In the present work the oxidizing treatments were performed at 500°C for varying times. The catalytic performances were compared in a flow microreactor. Catalysts characterization was achieved by surface area measurements, XRD, TGA coupled with DTA, UV–VIS spectroscopy, and ^{31}P NMR by spin echo mapping.

EXPERIMENTAL

Preparation of the Vanadyl Pyrophosphate

The precursor, $VO(HPO_4)$, $0.5H_2O$, was prepared according to the method given by Johnson *et al.* (22) by refluxing a suspension of V_2O_5 (11.8 g) in isobutanol (250 ml) in the presence of 85% H_3PO_4, with a ratio $P/V = 1.1$ for 16 h. The formation of the precursor was checked by XRD. The precursor was then heated (0.5°C min^{-1}) in a quartz tube under a nitrogen flow up to 750°C and kept at this temperature for 72 h.

Oxidizing Pretreatments

$(VO)_2P_2O_7$ prepared at 750°C, denoted PYRO, was heated up to 500°C (5°C min^{-1}) under an oxygen flow (20 ml/min) and then kept at this temperature for varying periods, from 0.5 to 24 h. We obtained therefore a series of oxidized samples, prepared from the same batch of $(VO)_2P_2O_7$, oxidized for different times. The mass of each sample was typically 1.5 g.

Catalytic Test

The catalytic performances of the oxidized pyrophosphate catalysts were compared at 380°C and at atmospheric pressure in a flow microreactor (mass of catalyst: 0.280 g) with the mixture composition: $C_4H_{10}/O_2/He$, 1.6/18/80.4, and a $GHSV = 1500\ h^{-1}$. Gas analysis was performed by on-line gas chromatography with automatically controlled sampling valves as previously described (19). Runs were conducted until a stationary state of the catalytic performances was achieved, in any case, at least about 20 h on stream. Carbon mass balance was better than 98%.

Catalyst Characterization

The specific surface area was measured by low-temperature nitrogen adsorption according to the BET method. TGA–DTA was performed under an oxygen flow (40 ml/min) in an automatic Setaram balance. XRD powder patterns were recorded with a Siemens diffractometer using the Cu $K\alpha$ radiation. Diffuse reflectance spectra in the absorbance mode were recorded using a Perkin–Elmer (UV–VIS) spectrometer. ^{31}P NMR spin echo mapping spectra have been recorded with a Brucker spectrometer.

RESULTS

Catalytic Performances

The changes in the selectivity for MA formation for the series of oxidized samples are illustrated in Fig. 1. With respect to the starting PYRO sample ($S_{MA} = 52\%$), a strong increase of selectivity occurs with a maximum (84%) corresponding to 1 h of oxidizing pretreatment (PYRO-OX-1). For longer times of pretreatment, the selectivity first slightly decreases down to 76% (PYRO-OX-3) and then tends to stabilize as shown in Fig. 1. It is noteworthy to say that selectivity was measured at constant conversion of *n*-butane: in the range 10–12% for every catalyst whatever the time of oxidizing pretreatment. This increase of selectivity for MA appears to result of a decrease in the CO_x formation, especially CO_2 which is no more detected on the oxidized samples. It may also be stressed that these improved catalytic performances are stable with time of reaction: the *n*-butane conversion, the selectivity for MA and CO remain the same from the very beginning of the run up to about 23 h on stream (the runs were usually not conducted that long).

The surface area of the starting PYRO sample was 7.8 $m^2\ g^{-1}$. The oxidized samples had a somewhat lower

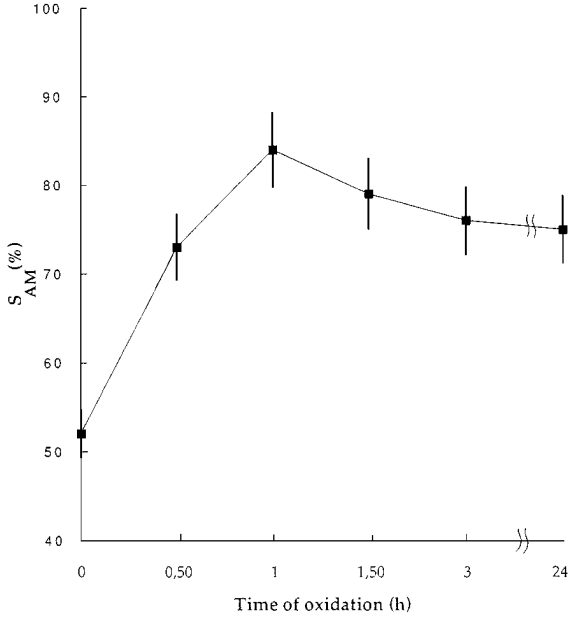

FIG. 1. MA selectivity (S_{MA}) as a function of time of oxidation pretreatment of the PYRO catalyst.

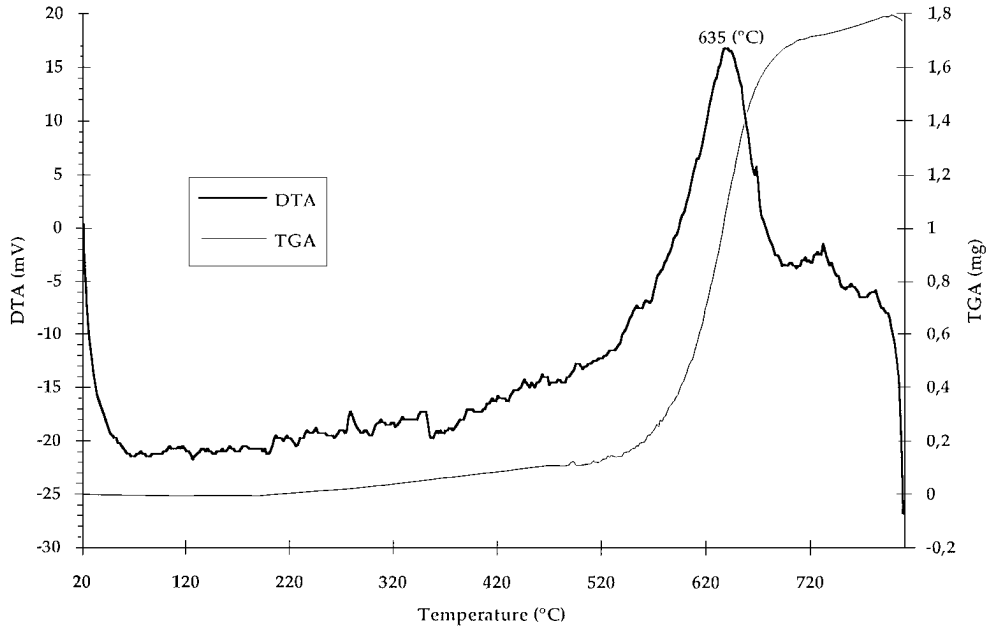

FIG. 2. DTA/TGA curves as a function of temperature under an oxygen flow.

surface area, in the range 5–7 $m^2\ g^{-1}$. The intrinsic activity for the conversion of *n*-butane on the starting PYRO sample was $V_i = 1.3 \times 10^{-8}$ mol $s^{-1}\ m^{-2}$. V_i increased only slightly for the oxidized samples. For example, $V_i = 1.5 \times 10^{-8}$ mol $s^{-1}\ m^{-2}$ for the catalyst denoted PYRO-OX-3. Considering the experimental accuracy, it may be concluded that oxidizing treatments do not significantly affect the activity of the PYRO catalyst.

As shown for example by Guliants *et al.* (6), most V^V orthophosphate phases have finite solubility in water and can be removed more or less completely by rinsing the catalyst with boiling water. Such a water washing was performed on PYRO-OX-3 and PYRO-OX-24 samples which recovered their initial color: gray–green instead of a yellowish color for oxidized samples. Such samples were then compared in the catalytic test. The *n*-butane conversion was unaffected, about 10%, but the selectivity for MA decreases from 76 to 68% for the PYRO-OX-3 sample and from 75 to 60% for the PYRO-OX-24 sample. These figures were measured after stabilization on stream for at least 20 h because we observed in that case a slight initial decrease of the selectivity for MA. Although the selectivity for MA is lowered for the water-washed samples, it remains significantly higher than for the starting PYRO catalyst.

CHARACTERIZATION

TGA–DTA Measurements

The mass of the PYRO catalyst in the platinum crucible was about 30 mg and the oxygen flow was 40 ml/min. In the first experiment, the temperature was linearly raised (5°C/min) from room temperature to 800°C. As shown in Fig. 2, oxidation readily occurs above about 550°C as evidenced by the increase of mass and the exothermic peak with a maximum at 635°C.

In a second experiment, the mass increase (Δm) due to oxidation was recorded under the same oxygen flow at a constant temperature, 500°C, for 24 h. No heat flow was recorded, in agreement with a slow oxidation process. The TGA curve showed that the mass increased nearly linearly with time: $\Delta m = 1.96\%$ for 24 h. As complete oxidation of $(VO)_2P_2O_7$ to $VOPO_4$ corresponds to a mass increase of 5.19%, a mass increase of 1.96% should be indicative of the formation of about 38% of $VOPO_4$. The present experiment demonstrates that the oxidation of $(VO)_2P_2O_7$ at 500°C actually occurred at a slow rate.

XRD Patterns

XRD patterns of typical oxidized samples are compared in Fig. 3A with the pattern of the starting PYRO catalyst which is characteristic of a pure and well-crystallized $(VO)_2P_2O_7$ phase with a high and narrow (200) reflection. With increasing time of oxidation, a general decrease of the intensity of the $(VO)_2P_2O_7$ diffraction peaks occurs as shown in Fig. 3A. This is especially the case for the (200) reflection.

The integral width *W* of the XRD lines may be used to characterize the extent of structural disorder, such as stacking faults (6, 23, 24). As shown in Fig. 4, the changes with time of oxidation of *W*(200) follow an opposite trend to those of *W*(032) and *W*(024). This observation suggests that,

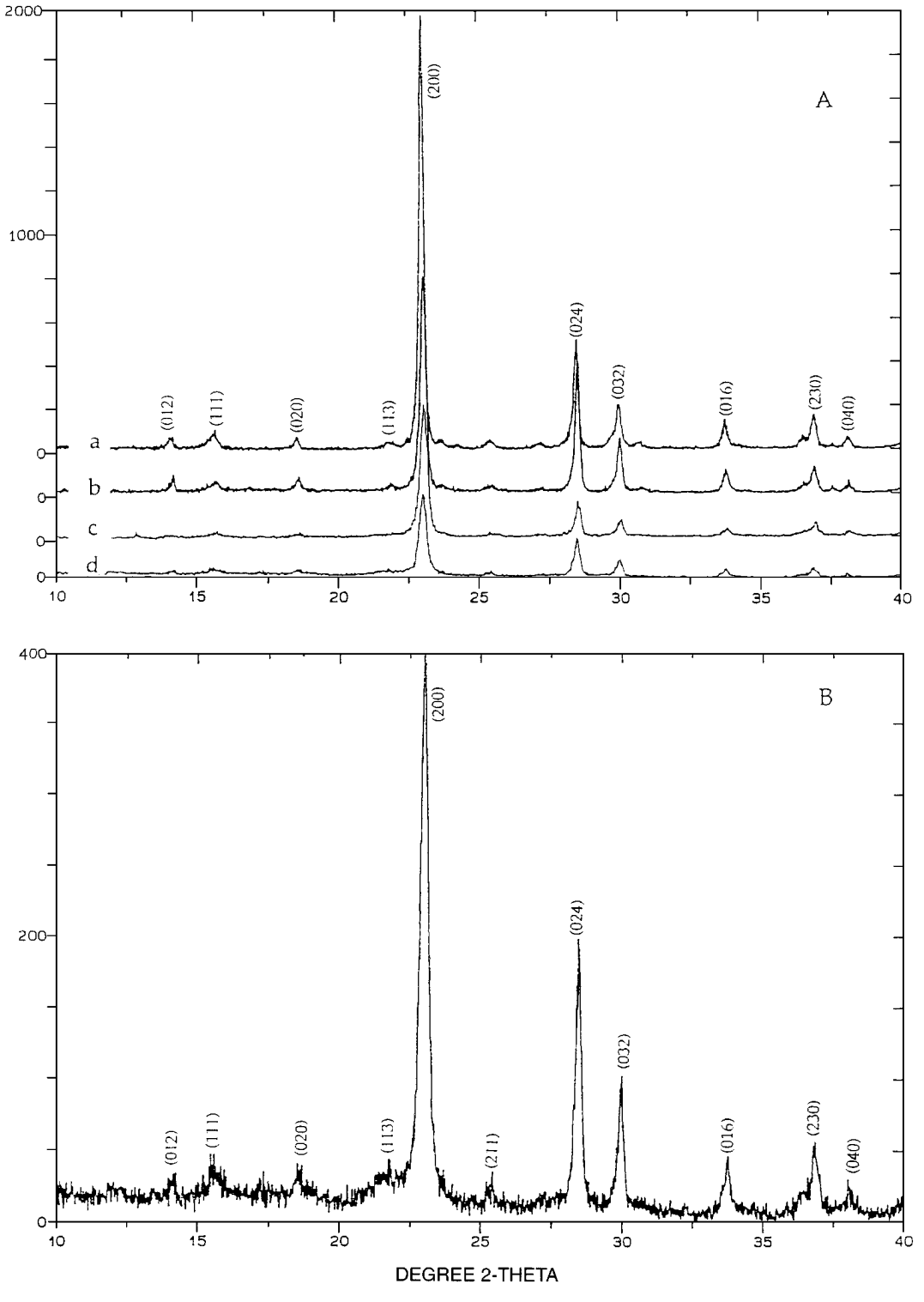

FIG. 3. XRD patterns. (A) The vanadyl pyrophosphate catalyst before any oxidation treatments (a) and after an oxidation treatment of 1 h (b), 3 h (c), and 24 h (d). (B) Spectrum (d) at a magnified scale.

for times of oxidation up to 3 h, there is an increasing preferential structural disorder along the [100] axis, whereas this phenomenon is not observed in directions normal to the (100) faces.

The pattern corresponding to PYRO-OX-24 (pattern d in Fig. 3A) is shown with a magnified scale in Fig. 3B. Despite the long oxidizing treatment (24 h), all the diffraction peaks can still be attributed to $(VO)_2P_2O_7$. Note however

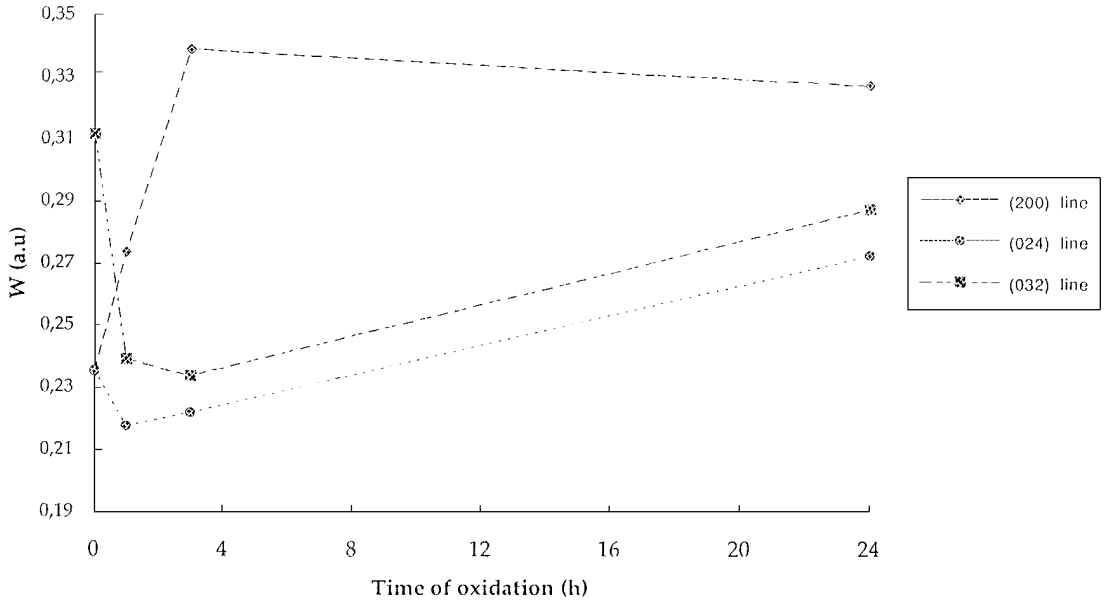

FIG. 4. Changes with time of oxidation of the integral width of (200), (024), and (032) XRD lines.

the presence of a background which may indicate the presence of some amorphous phase in connection with structural disorder.

It is surprising that XRD patterns only show the lines of $(VO)_2P_2O_7$ with no evidence for the formation of crystalline $VOPO_4$ phase. Indeed, XRD is not very sensitive to the detection of $VOPO_4$ in $(VO)_2P_2O_7$. According to Cavani *et al.* (23) there may be as high as 20% of $VOPO_4$ in addition of $(VO)_2P_2O_7$ with no clear modification of the XRD pattern. However, we believe that a relative amount of 37% of $VOPO_4$, as suggested by TGA measurements, can be discarded. The kinetics of oxidation in the preparation reactor was most likely slower than in the TGA balance, probably as a result of the much more important mass of solid (1.5 g instead of about 0.030 g), the oxygen flow (20 ml/min instead of 40 ml/min) and the depth of the bed (about 12 mm instead of 5 mm, respectively). It will be shown later that NMR analysis allowed us to confirm that the kinetics of oxidation was actually slower in the preparation tube.

Diffuse Reflectance Spectra

We mainly focused on the charge-transfer (CT) band near 300 nm which is known to be sensitive to the presence of V^V species (23, 25). Figure 5A shows that the width of this band becomes broader and broader with time of oxidizing pretreatment. If we assume that the oxidation is restricted to the near surface region, the initial V^{IV} content remains roughly constant and the relative amount of V^V can be estimated by substracting the area (A) under the band of oxidized catalysts from the area (A_O) under the band of the starting PYRO sample where only V^{IV} is present. Figure 5B shows that the V^V amount estimated in this way first increases rapidly with time of oxidation and then tends to level off. After water washing, the spectrum relative to PYRO-OX-24 (d in Fig. 5A) was very similar to the spectrum of the starting PYRO catalyst (a in Fig. 5A). Clearly washing removes the CT band relative to V^V species in the 300–400 nm range and only the original CT band near 250–300 nm typical of V^{IV} species remains. The shape and intensity of this band are quite similar to the band recorded on the PYRO sample before any oxidation treatment. This observation again suggests that the oxidation was less deep and important than suggested by TGA measurements.

^{31}P NMR Spin Echo Mapping Spectra

Figure 6 compares the spectra of the starting PYRO catalyst (a) and the catalyst oxidized for 24 h (b). Spectrum (a), with a peak at about 2,700 ppm, is typical of a pure and well-crystallized $(VO)_2P_2O_7$ phase, in agreement with previous studies on V–P–O catalysts by this technique (12, 26, 27). The lack on any signal around 0 ppm is noteworthy because it indicates the absence of V^{5+} (or at least a nondetectable concentration). This is indeed not the case for spectrum (b) which exhibits an additional peak near 0 ppm. In previous work (12), we have shown that the relative bulk concentration of V^{5+} can be estimated on the basis of the area under the V^{5+} and the V^{4+} peaks. This measurement yields a relative amount of V^{5+} close to 13%. As already suggested by XRD and diffuse reflectance spectra, NMR analysis then confirms that the kinetics of oxidation of $(VO)_2P_2O_7$ in the preparation tube was slower than in the small crucible used for TGA–DTA measurements.

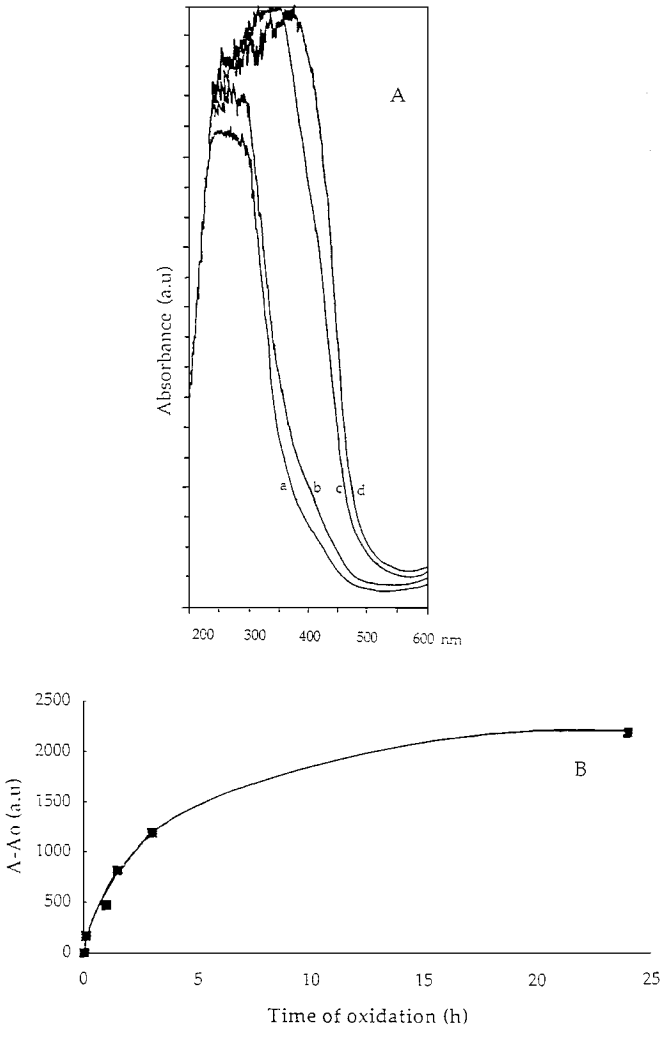

FIG. 5. (A) UV–VIS (spectra charge transfer band) of the vanadyl pyrophosphate catalyst before any oxidation treatment (a) and after an oxidation treatment of 1 h (b), 3 h (c), and 24 h (d). (B) Area difference ($A - A_0$) under the UV–VIS CT bands shown in Fig. 5A: Estimation of the relative V^V amount (see the text).

DISCUSSION AND CONCLUSIONS

In previous work (12), we have shown that an excess of V^V sites is detrimental for the catalytic performances because it favors CO_x formation. This conclusion is in line with the model developed by Cavani *et al.* (28) who explained that the MA selectivity goes through a maximum for a given degree of surface oxidation that is a given V^V/V_{total} ratio. Such a model is in agreement with the concept of site isolation first proposed by Callahan and Grasselli (29): selective oxidation would require an optimal number of active oxygen species near the adsorbed hydrocarbon.

V^V sites are most likely involved in the oxygen insertion steps (1–3, 10–12) and their increased density on oxidized pyrophosphate samples can therefore explain the striking improvement in MA selectivity observed in the present work. However, besides their number, the nature of the V^V species could also be important. For example, Cavani and Trifirò (3) claimed that, besides V^V sites involved in selective oxidation, other kinds of V^V species would be responsible for the direct oxidation of *n*-butane into CO_x and others active in the overoxidation of MA.

Following this general discussion, it can be concluded that the oxidation of vanadyl pyrophosphate at 500°C leads to the formation of selective V^V species responsible for the MA selectivity increase up to a maximum which would correspond to an optimal density (28) of active surface oxygen species, capable of the redox reaction of oxygen insertion (30). Owing to the crystalline structure of $(VO)_2P_2O_7$ with platelets exposing mainly the (100) cleavage plane, the oxidation process is anisotropic (10, 18) and selective V^V species are most likely located in the (100) face because side faces are nonselective for *n*-butane oxidation to MA.

The improvement in MA selectivity is quite significant (Fig. 1) and is not transient as shown in catalytic runs extending up to about 23 h. However, the activity of the catalyst is not significantly modified, which shows that the number of sites responsible for the activation of *n*-butane has not changed and that V^V sites would not be directly involved in this process. Recall that the activation of *n*-butane has been correlated with the presence of V^{IV} Lewis acidic sites (31–33). From electrical conductivity measurements (34), we recently proposed that butane activation would require V^{IV} sites associated with O^- species.

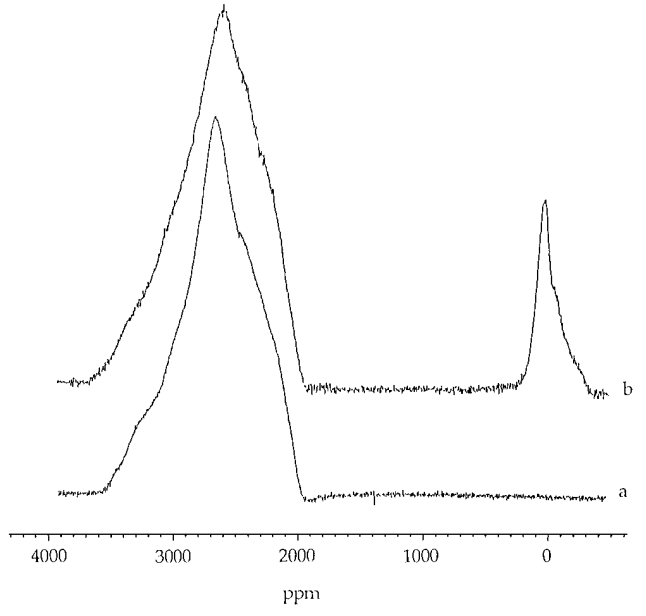

FIG. 6. ^{31}P NMR spin echo spectra of (a) the starting $(VO)_2P_2O_7$ PYRO sample and (b) the same sample oxidized at 500°C for 24 h.

It is noteworthy that the increase of selectivity on oxidized sample is mainly correlated with a decrease of selectivity to CO_2 (the formation of which is virtually suppressed) and not to CO. This could be interpreted by the fact that the direct oxidation of butane to CO_2 is inhibited on oxidized catalysts. In a previous study (19), we have shown that this is the preferential route to CO_x formation. However, Igarashi *et al.* (35) concluded that the consecutive overoxidation of MA is limiting the selectivity when the conversion increases. Therefore, the enhancement in MA selectivity could also be explained by some inhibition of the MA overoxidation. According to Schuurman and Gleaves (15), the MA molecule is more weakly adsorbed on the oxidized pyrophosphate and therefore will desorb more easily.

TGA, UV–VIS, and NMR spectroscopies have shown that the pyrophosphate samples are slowly oxidized at 500°C under oxygen. According to the estimation based on ^{31}P NMR spin echo mapping spectra, the total amount of V^{5+} reaches about 13% after an oxidation treatment for 24 h. Assuming 8.4 μmol/m^2 of vanadium on the surface of $(VO)_2P_2O_7$ (36) and considering a specific surface of 5 m^2/g, this amount of V^{5+} corresponds to about 20 monolayers. Nevertheless, the lines typical of any crystallized $VOPO_4$ phase have not been detected by XRD (Fig. 3). These observations could indicate the formation of V^{5+} domains either amorphous or too small to assume the long range order of any $VOPO_4$ phase.

However, one must not forget that oxidation also induced the anisotropic creation of structural disorder as evidenced by the preferential broadening of the (200) reflection. Structural defects have been previously detected by XRD (37, 38), magnetic susceptibility (39, 40), EXAFS (41), and HREM (42). In the recent paper of Nguyen *et al.* (38), the presence of extended defects has been associated with V^{5+} in the bulk of $(VO)_2P_2O_7$ rather than V^{5+} in an additional $VOPO_4$ phase, in agreement with previous magnetic susceptibility data (39, 40). Nguyen *et al.* also found that the XRD pattern of $(VO)_2P_2O_7$ was preserved, despite the presence of V^{5+} defects, as in the present work.

Therefore, it may be proposed that the enhancement of selectivity for MA formation results from the creation, by the oxidation treatment at 500°C, of both bulk and surface V^{5+} also acting as structural defects in the $(VO)_2P_2O_7$ lattice. The presence of these reactive V^{5+} species would be crucial for the oxygen insertion steps of the reaction, especially the last step from furan to MA as concluded by Rodemerck *et al.* in a very recent paper (43). The fact that, after water washing of the oxidized catalyst, the samples still display a MA selectivity higher than the value measured on the starting PYRO catalyst should imply that reactive V^{5+} defects have not been completely removed by water leaching.

It may be added that the presence of V^{5+} within a significant number of sublayers also means that a corresponding amount of oxygen could be stored in the $(VO)_2P_2O_7$ lattice before the formation of a definite crystalline $VOPO_4$ phase. López-Granados *et al.* (41) already proposed the presence of interstitial oxygen in the pyrophosphate lattice. Oxygen storage within a few surface layers has been also invoked in oxygen-treated V–P–O catalysts by Schuurman *et al.* (14).

Finally the use of other techniques appears to be necessary to gain more information on the nature of V^{5+} species which are most likely responsible for the strong increase of selectivity to MA. This will be the aim of a forthcoming publication based on electrical conductivity, Raman spectroscopy, NMR, and XPS characterization.

ACKNOWLEDGMENTS

We are indebted to Dr. A. Tuel for his assistance in the NMR analysis. We thank Dr. G. Coudurier for helpful discussions on the UV–VIS spectra. We are also grateful to Mr. V. Martin for his assistance in the TGA–DTA experiments.

REFERENCES

1. Centi, G., Trifirò, F., Ebner, J. R., and Franchetti, V. M., *Chem. Rev.* **88**, 55 (1988).
2. Centi, G., *Catal. Today* **16**, 5 (1993). [and other papers in this special issue devoted to "Vanadyl Pyrophosphate Catalysts"]
3. Cavani, F., and Trifirò, F., *Catalysis* **11**, 246 (1994).
4. Ebner, J. R., and Thompson, M. R., *Catal. Today* **16**, 51 (1993).
5. Trifirò, F., *Catal. Today* **16**, 91 (1993).
6. Guliants, V. V., Benziger, J. B., Sundaresan, S., Wachs, I. E., Jehng, J. M., and Roberts, J. E., *Catal. Today* **28**, 275 (1996).
7. Bordes, E., and Contractor, R. M., *Topics Catal.* **3**, 365 (1996).
8. Centi, G., Golinelli, G., and Trifirò, F., *Appl. Catal.* **48**, 13 (1989).
9. Ben Abdelouabab, F., Olier, R., Guillaume, N., Lefèbvre, F., and Volta, J. C., *J. Catal.* **134**, 151 (1992).
10. Volta, J. C., Béré, K., Zhang, Y. J., and Olier, R., *in* "Catalytic Selective Oxidation" (S. T. Oyama and J. W. Hightower, Eds.), ACS Symposium Series 523, p. 217. Am. Chem. Soc., Washington, DC, 1993.
11. Hutchings, G. J., Desmartin-Chomel, A., Olier, R., and Volta, J. C., *Nature* **368**, 41 (1994).
12. Abon, M., Béré, K. E., Tuel, A., and Delichère, P., *J. Catal.* **156**, 28 (1995).
13. Hutchings, G. J., and Higgins, R., *J. Catal.* **162**, 153 (1996).
14. Schuurman, Y., Gleaves, J. T., Ebner, J. R., and Mummey, M. J., *in* "New Developments in Selective Oxidation" (V. C. Corberan and S. V. Bellon, Eds.), Vol. II, p. 203. Elsevier, Amsterdam, 1994.
15. Schuurman, Y., and Gleaves, J. T., *Ind. Eng. Chem. Res.* **33**, 2935 (1994).
16. Coulston, G. W., Bare, S. R., Kung, H., Birkeland, K., Bethke, G. K., Harlow, R., Herron, N., and Lee, P. L., *Science* **275**, 191 (1997).
17. Koyano, G., Okuhara, T., and Misono, M., *Catal. Lett.* **32**, 205 (1995).
18. Koyano, G., Yamaguchi, F., Okuhara, T., and Misono, M., *Catal. Lett.* **41**, 149 (1996).
19. Zhang-Lin, Y., Forissier, M., Sneeden, R. P., Védrine, J. C., and Volta, J. C., *J. Catal.* **145**, 256 (1994).
20. Okuhara, T., Inumaru, K., and Misono, M., *in* "Catalytic Selective Oxidation" (S. T. Oyama and J. W. Hightower, Eds.), ACS Symposium Series, p. 156. Am. Chem. Soc., Washington, DC, 1993.
21. Ziolkowski, J., Bordes, E., and Courtine, P., *J. Catal.* **122**, 126 (1990).
22. Johnson, J. W., Johnston, D. C., Jacobson, A. J., and Brody, J. F., *J. Am. Chem. Soc.* **106**, 8123 (1984).

23. Cavani, F., Centi, G., Manenti, I., and Trifirò, F., *Ind. Eng. Chem. Prod. Res. Dev.* **24**, 221 (1985).
24. Igarashi, H., Tsuji, K., Okuhara, T., and Misono, M., *J. Phys. Chem.* **93**, 7065 (1993).
25. Cavani, F., Centi, G., Trifirò, F., and Vaccari, A., *in* "Adsorption and Catalysis on Oxide Surfaces" (M. Che and G. C. Bond, Eds.), p. 287. 1985.
26. Li, J., Lashier, M. E., Schrader, G. L., and Gerstein, B. C., *Appl. Catal.* **73**, 83 (1991).
27. Sananes, M. T., Tuel, A., and Volta, J. C., *J. Catal.* **145**, 251 (1994).
28. Cavani, F., Centi, G., Trifirò, F., and Grasselli, R. K., *Catal. Today* **3**, 185 (1988).
29. Callahan, J. L., and Grasselli, R. K., *AlCHE* **9**, 755 (1963).
30. Abon, M., Béré, K. E., and Delichère, P., *Catal. Today* **33**, 15 (1997).
31. Busca, G., Centi, G., and Trifirò, F., *Appl. Catal.* **25**, 265 (1986).
32. Cornaglia, L. M., Lombardo, E. A., Anderson, J. A., and Garcia-Fierro, J. L., *Appl. Catal. A* **100**, 37 (1993).
33. Béré, K. E., Gravelle, M., and Abon, M., *J. Chim. Phys.* **92**, 1521 (1995).
34. Herrmann, J. M., Vernoux, P., Béré, K. E., and Abon, M., *J. Catal.* **167**, 106 (1997).
35. Igarashi, H., Tsuji, K., Okuhara, T., and Misono, M., *J. Phys. Chem.* **97**, 7065 (1993).
36. Satsuma, A., Tanaka, Y., Hattori, A., and Murakami, Y., *J. Chem. Soc., Chem. Commun.* 1073 (1994).
37. Cavani, F., Centi, G., and Trifirò, F., *J. Chem. Soc. Chem. Commun.* 492 (1985).
38. Nguyen, P. T., Sleight, A. W., Roberts, N., and Warren, W. W., *J. Solid State Chem.* **122**, 259 (1996).
39. Johnston, D. C., and Johnson, J. W., *J. Chem. Soc. Chem. Commun.* 1720 (1985).
40. Johnson, J. W., Johnston, D. C., Jacobson, A. J., and Brody, J. F., *J. Am. Chem. Soc.* **106**, 8123 (1984).
41. López-Granados, M., Conesa, J. C., and Fernandez-Garcia, M., *J. Catal.* **141**, 671 (1993).
42. Gai, P. L., and Kourtakis, K., *Science* **267**, 661 (1995).
43. Rodemerk, U., Kubias, B., Zanthoff, H. W., Wolf, G. U., and Baerns, *Appl. Catal. A* **153**, 217 (1997).